TISSUE ENGINEERING: Part C
Volume 25, Number 10, 2019

DOI: 10.1089/ten.tec.2019.0116

termis
Tissue Engineering
& Regenerative Medicine
International Society

METHODS ARTICLE

A Systematic Review and Guide to Mechanical Testing for Articular Cartilage Tissue Engineering

Jay M. Patel, PhD,[1,2] Brian C. Wise, MS,[1,3] Edward D. Bonnevie, PhD,[1,2] and Robert L. Mauck, PhD[1–3]

Articular cartilage is integral to the mechanical function of many joints in the body. When injured, cartilage lacks the capacity to self-heal, and thus, therapies and replacements have been developed in recent decades to treat damaged cartilage. Given that the primary function of articular cartilage is mechanical in nature, rigorous physical evaluation of cartilage tissues undergoing treatment and cartilage constructs intended for replacement is an absolute necessity. With the large number of groups developing cartilage tissue engineering strategies, however, a variety of mechanical testing protocols have been reported in the literature. This lack of consensus in testing methods makes comparison between studies difficult at times, and can lead to misinterpretation of data relative to native tissue. Therefore, the purpose of this study was to systematically review mechanical testing of articular cartilage and cartilage repair constructs over the past 10 years (January 2009–December 2018), to highlight the most common testing configurations, and to identify key testing parameters. For the most common tests, key parameters identified in this systematic review were validated by characterizing both cartilage tissue and hydrogels commonly used in cartilage tissue engineering. Our findings show that compression testing was the most common test performed (80.2%; 158/197), followed by evaluation of frictional properties (18.8%; 37/197). Upon further review of those studies performing compression testing, the various modes (ramp, stress relaxation, creep, dynamic) and testing configurations (unconfined, confined, *in situ*) are described and systematically reviewed for parameters, including strain rate, equilibrium time, and maximum strain. This systematic analysis revealed considerable variability in testing methods. Our validation testing studies showed that such variations in testing criteria could have large implications on reported outcome parameters (e.g., modulus) and the interpretation of findings from these studies. This analysis is carried out for all common testing methods, followed by a discussion of less common trends and directions in the mechanical evaluation of cartilage tissues and constructs. Overall, this work may serve as a guide for cartilage tissue engineers seeking to rigorously evaluate the physical properties of their novel treatment strategies.

Keywords: cartilage, mechanical testing, systematic review, compression, biomechanics

Impact Statement

Articular cartilage tissue engineering has made significant strides with regard to treatments and replacements for injured tissue. The evaluation of these approaches typically involves mechanical testing, yet the plethora of testing techniques makes comparisons between studies difficult, and often leads to misinterpretation of data compared with native tissue. This study serves as a guide for the mechanical testing of cartilage tissues and constructs, highlighting recent trends in test conditions and validating these common procedures. Cartilage tissue engineers, especially those unfamiliar with mechanical testing protocols, will benefit from this study in their quest to physically evaluate novel treatment and regeneration approaches.

[1]McKay Orthopedic Research Laboratory, Perelman School of Medicine, University of Pennsylvania, Philadelphia, Pennsylvania.
[2]Translational Musculoskeletal Research Center, Corporal Michael J Crescenz VA Medical Center, Philadelphia, Pennsylvania.
[3]Department of Bioengineering, University of Pennsylvania, Philadelphia, Pennsylvania.

Introduction

ARTICULAR CARTILAGE IS a remarkable, complex tissue that is instrumental for load bearing, shock absorption, and articulation of joints throughout the body.[1] Healthy articular cartilage experiences a complex loading environment, including compression, shear, friction, and tension.[1,2] The distinct and precise composition and organization of the cartilage extracellular matrix (ECM; Fig. 1A) allows it to resist these stresses through poroviscoelastic mechanisms,[3] where fluid pressurization and stress dissipation occur in a time-dependent manner.[4] Injury and degeneration of articular cartilage compromises its load-bearing capabilities,[5,6] and due to the lack of vascularity in the tissue, there is limited self-healing to restore mechanical function.[7] Current repair and replacement strategies, such as microfracture,[8,9] autologous chondrocyte implantation,[10,11] autologous cultured chondrocytes on porcine collagen membrane (MACI), and autologous matrix-induced chondrogenesis[12] have made strides in terms of providing symptomatic relief, but long-term outcomes are inconsistent,[11,13] potentially due to inadequate mechanical function of the repair tissue. Therapeutics, such as nonsteroidal anti-inflammatory drugs, corticosteroids, and hyaluronic acid, can also provide short-term symptomatic relief, but do not restore chondrocyte or ECM function, and are cleared from the joint within days.

Consequently, the last three decades have focused on the combination of materials, cells, and factors to either slow the degeneration of cartilage or to replace the tissue altogether.[14] To evaluate such approaches, scientists, engineers, and clinicians turn toward a host of *in vitro*, *in situ*, *in vivo*, and *ex vivo* outcome measures. The most frequent assays are biological in nature (e.g., biochemical composition, gene expression, or histology[15,16]). However, to quantify the mechanical function of the repaired or treated tissue, evaluation of the physical properties of the tissues is essential.[17–19] Unfortunately, there are a variety of mechanical tests (Fig. 1B) and widely varying protocols for each type of test.[17] This lack of standardization in testing methods and evaluation leads to variability in reported outcome metrics, inability to compare directly between different studies, and increases the likelihood for

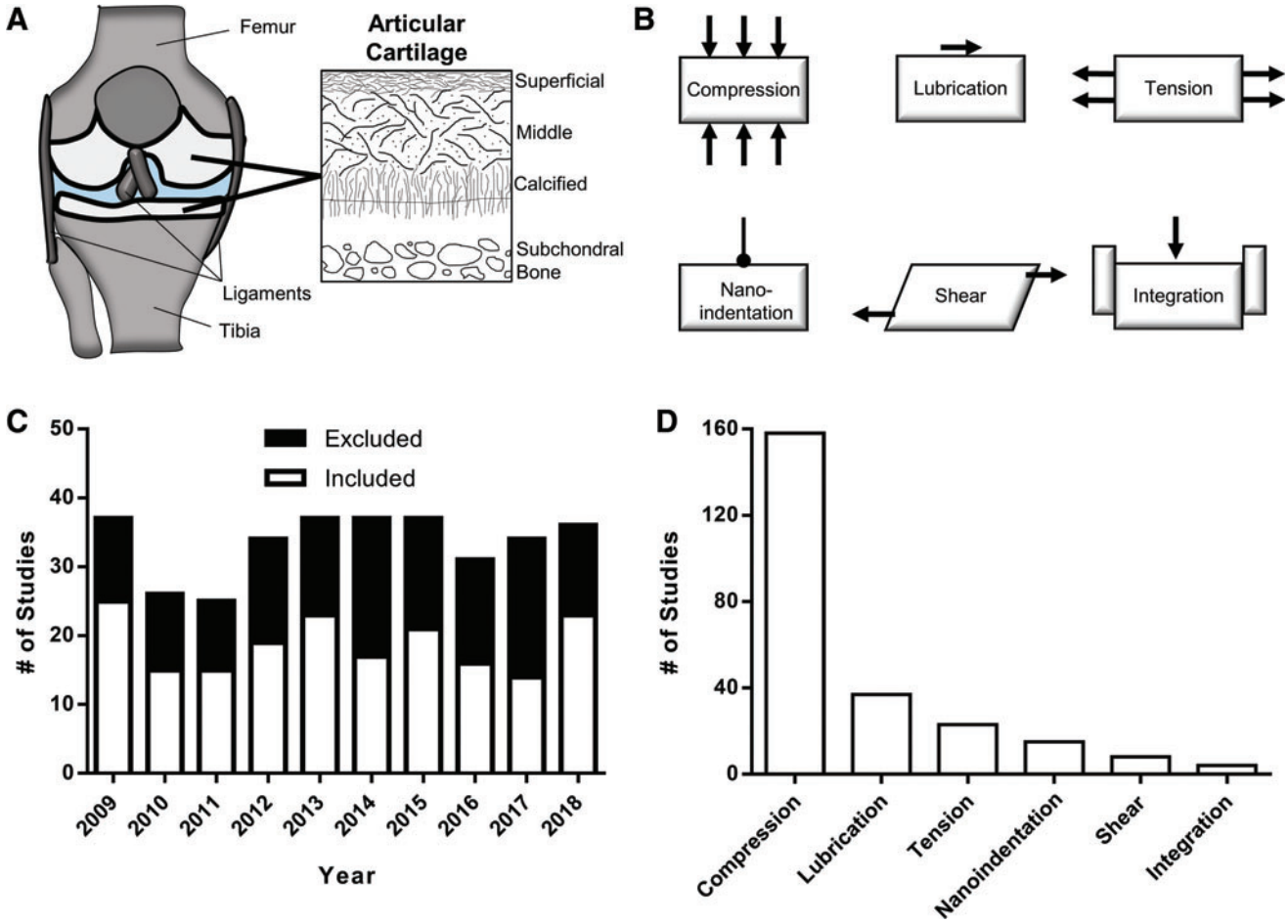

FIG. 1. **(A)** Anatomy of the knee joint, showing the femur, tibia, and ligaments, with articular cartilage (in *white*). Schematic of articular cartilage architecture showing anisotropic alignment of collagen bundles. **(B)** Schematics of common modes of articular cartilage mechanical testing (compression, lubrication, tension, nanoindentation, shear, integration). **(C)** Systematic review of ''articular cartilage mechanical testing'' from 2009 to 2018, showing excluded and included studies. **(D)** Breakdown of testing type ($n = 197$ studies), showing the overwhelming majority of studies (80.2%; 158/197) reporting data from compression testing. Color images are available online.

misinterpretation of mechanical data relative to native tissue.

Therefore, the purpose of this study was to aggregate the literature on cartilage mechanical testing procedures and to perform validation studies of these testing protocols. Specifically, we (1) systematically review articular cartilage mechanical testing studies from the last 10 years; (2) highlight trends in testing configurations and protocols; and (3) perform validation and comparison of the most common protocols. The intent of this work is to provide a primer for the interpretation of mechanical testing data and a resource for mechanical testing of both articular cartilage constructs and tissues.

Systematic Review of Articular Cartilage Mechanical Testing

To systematically review the last 10 years of studies that performed physical evaluation of cartilage tissue and constructs, a PubMed search with the terms ''Articular Cartilage Mechanical Testing'' was performed, focusing on the time period from January 2009 to December 2018. The search yielded a total of 348 articles (≥25/year), of which 197 (56.6%) were included in this systematic review (Fig. 1C and Supplementary Table S1). Common exclusion criteria were review articles (11 studies), finite element modeling studies (20 studies), meniscus tissue engineering studies (11 studies), and most frequently a lack of cartilage mechanical testing. Of the 197 studies to perform mechanical testing of cartilage tissue or constructs, the overwhelming majority performed compression testing (158/197; 80.2%), followed by lubrication (37/197; 18.8%), followed by tension, nanoindentation, shear, and integration testing (Fig. 1D). Since the majority of studies carried out compression testing, the various compression testing configurations and methods were further reviewed and validated.

From the 158 compression studies, three major testing configurations were noted: unconfined, confined, and *in situ* (Fig. 2A). Both unconfined and confined compression involve testing a stand-alone sample of cartilage tissue or construct, either between two impermeable platens (unconfined) or within an impermeable chamber. Confined compression then involves the use of a porous metal indenter (or impermeable indenter with porous chamber) to allow for fluid flow out of the tissue. Finally, *in situ* testing involves testing locally on a whole cartilage sample, often an entire osteochondral specimen. These specimens are commonly embedded in a rigid fixture, and compression is applied through a porous or nonporous indenter.

Within these testing configurations, four testing protocols were commonly observed: ramp, stress relaxation, creep, and dynamic (Fig. 2B). Ramp testing involves applying deformation (strain) at a constant rate, while simultaneously measuring the stress response. Stress relaxation involves applying a strain to a target level, and then holding the strain constant at that level, during which time the stress peaks and then relaxes to an equilibrium level. Creep involves the rapid application of a stress, which is then held constant, and the measurement of continued sample deformation (strain) with time. Finally, dynamic tests involve applying either a cyclic stress or strain, and measuring the corresponding response.

Of the studies performing compression testing, nearly two-thirds (103/158) utilized an unconfined configuration, while only 15 studies utilized a confined chamber (Fig. 2C). Review of testing methods showed that ramp and stress relaxation testing were the most commonly performed. When testing method was broken down by configuration (Fig. 2D, E), it was apparent that an unconfined configuration was the most utilized for all tests, except for creep testing, which showed a tendency toward the use of confined (5/20) and *in situ* (13/20) modalities.

Compression Testing Review

The following section discusses the aforementioned compression tests (ramp, stress relaxation, creep, dynamic) in further detail. Cartilage tissue experiences forces normal (perpendicular) to the articulating surface, especially in load-bearing joints. Healthy articular cartilage can absorb rapid, near-instantaneous stresses through its fluid pressurization capacity; when loaded, the rise in interstitial fluid pressure and relatively low permeability of the tissue allows for compressive resistance.[1,20] Thus, testing parameters (e.g., testing rate and duration[21,22]) can have an impact on these load-bearing properties, and were reviewed from the corresponding literature, followed by validation testing to explore the effect of these key parameters on reportable outcomes.

To further characterize both tissue and construct properties, we utilized juvenile bovine trochlear cartilage and agarose hydrogels. Cartilage plugs (8 mm-diameter) were excised from trochlea, and were cut with a freezing stage microtome to isolate the cartilage transitional zone with parallel faces for testing. Agarose (2-hydroxyethylagarose) was dissolved at 3% w/v in deionized H_2O at 65°C, cast into six-well plates, and allowed to solidify by cooling. Agarose plugs (8 mm-diameter) were excised from well plates with a surgical biopsy punch. Samples were hydrated for at least 60 min before testing.

Ramp mechanical testing

Perhaps the easiest compressive test to perform on cartilage constructs and tissues is the ramp test, which involves the application of a constant compressive strain until a specified strain level is reached. However, the rate at which samples are compressed (Fig. 3A) can have a significant impact on the response of cartilage tissues and constructs,[23] as does the strain at which the tangent modulus (slope) is calculated (Fig. 3B). Thus, strain rate and strain at calculation were reviewed systematically. Of the 79 occurrences of ramp testing, 52 utilized a deformation rate (Fig. 3C; mm/s) and 24 utilized an actual strain rate (Fig. 3D; %/s), indicating that less than one-third of studies normalize the strain rate to sample thickness. While no differences were observed in strain rate between cartilage tissues and scaffolds/constructs, the highest strain rate was >100,000 times higher than the lowest rate, demonstrating that no consensus exists on the appropriate rate at which to test samples.

With regard to the ramp strain utilized in studies, 45/79 reported a value of either maximum strain or strain used for analysis (Fig. 3E). While not statistically different ($p = 0.0592$), scaffolds and constructs ($33.36\% \pm 25.08\%$) were tested to more than twice the compressive strain that cartilage tissue was tested to ($16.42\% \pm 10.41\%$). In fact, while only 1/12 of the studies testing cartilage compressed tissue to more than 20% strain, 16/33 studies testing constructs

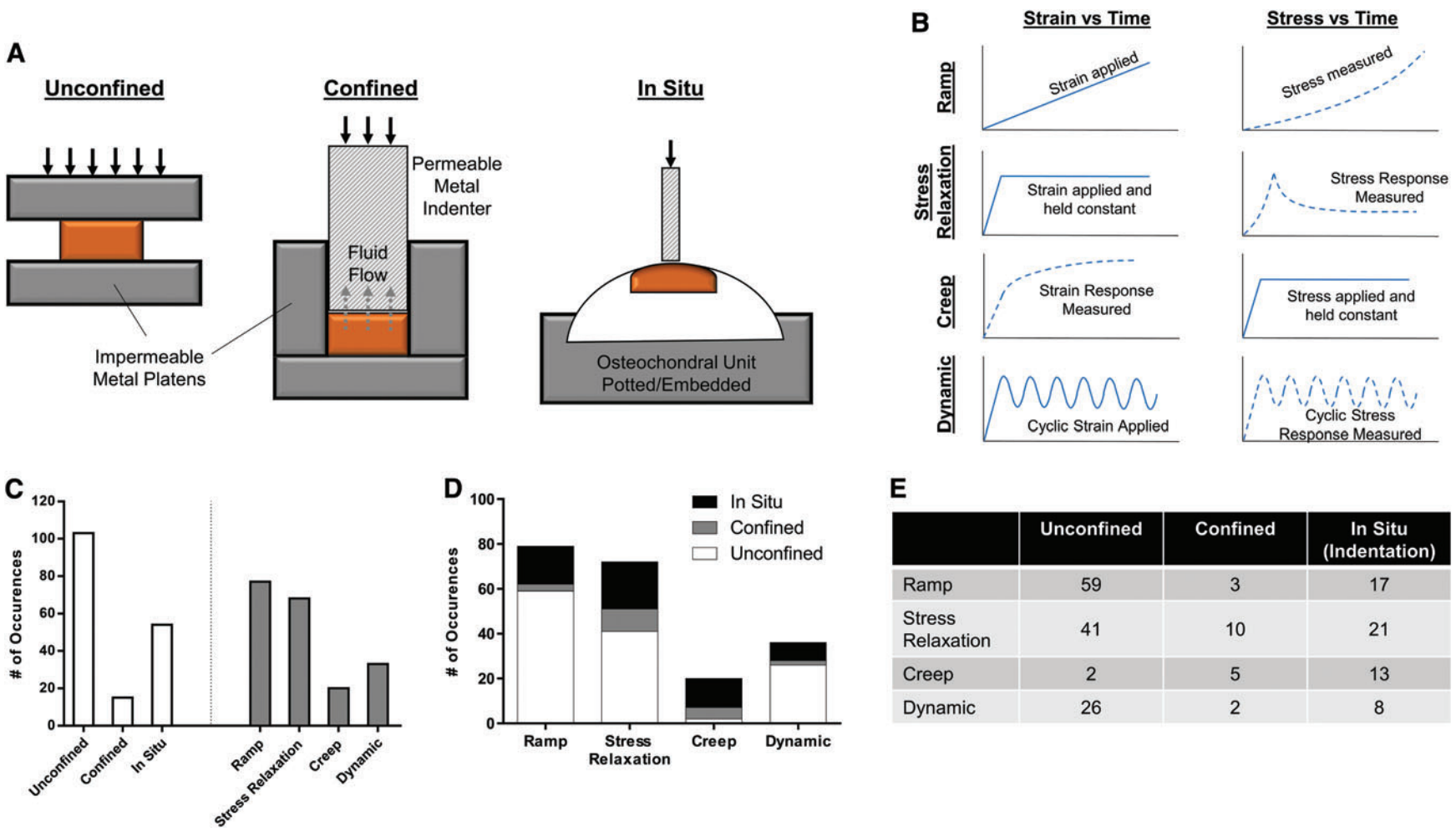

E

	Unconfined	Confined	In Situ (Indentation)
Ramp	59	3	17
Stress Relaxation	41	10	21
Creep	2	5	13
Dynamic	26	2	8

FIG. 2. Compression testing configurations and modes. **(A)** Testing configuration includes unconfined, confined, and *in situ* (indentation) testing. **(B)** Testing modes (ramp, stress relaxation, creep, dynamic) depend on strain versus time and stress versus time. **(C)** Number of occurrences of testing configurations and modes from systematic review. **(D, E)** Number of occurrences of each testing mode, separated by configuration type. Color images are available online.

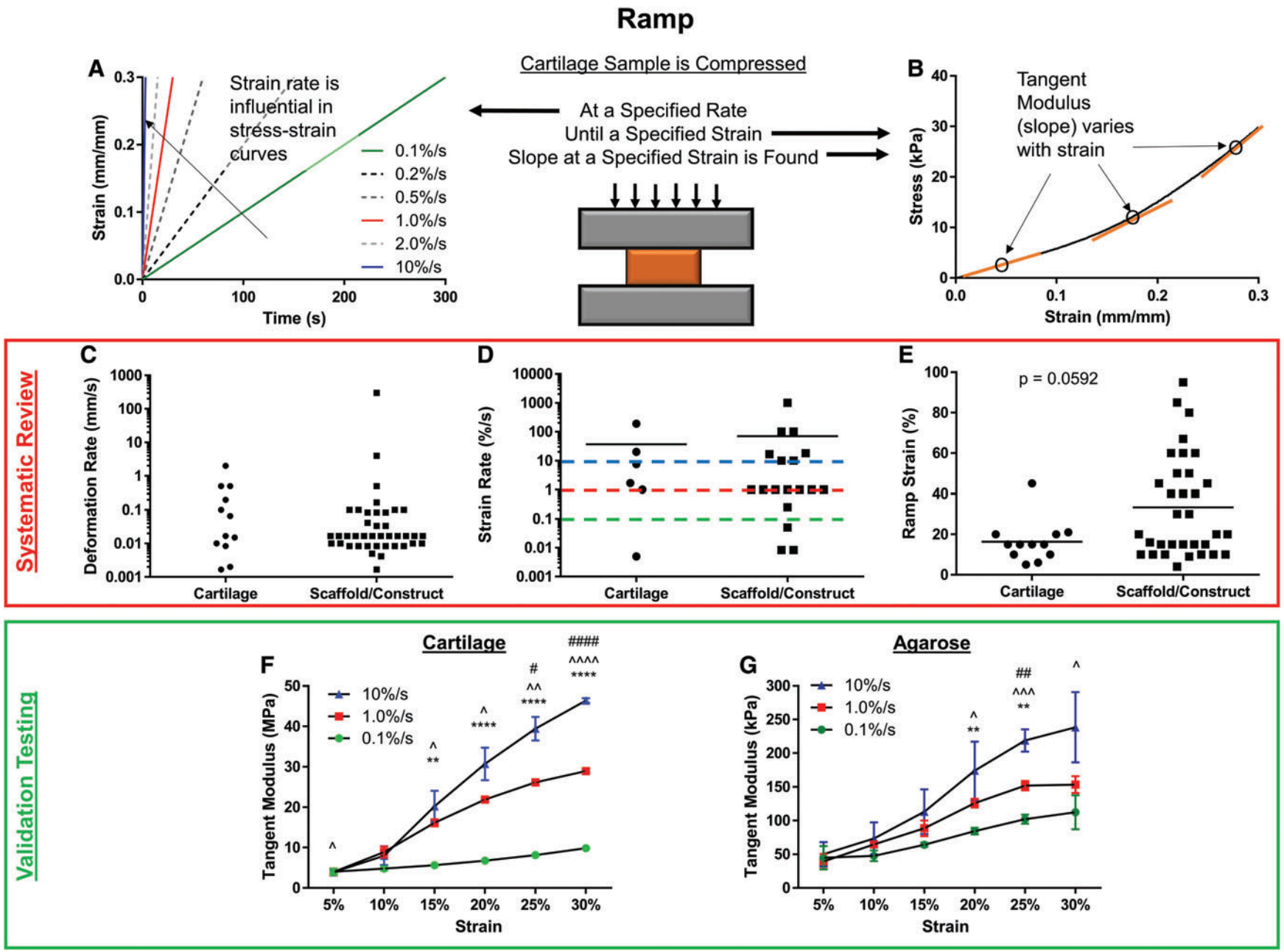

FIG. 3. Ramp testing. Cartilage samples can be compressed at **(A)** a variety of strain rates, and **(B)** tested to or analyzed at a variety of specified strains. The strain at which slope is determined can also impact the outcome values. Systematic review of **(C)** deformation rate (mm/s), **(D)** strain rate (%/s), and **(E)** ramp strain (%), split by cartilage tissue and scaffolds/constructs. Tangent modulus from validation testing of **(F)** cartilage and **(G)** agarose at three different strain rates (0.1, 1.0, and 10%/s), found at six different strains (5–30%). Mean ± standard deviation. Significant differences within strains are noted by * (0.1 vs. 1.0), ∧ (0.1 vs. 10), and # (1.0 vs. 10), with the number of symbols (1, 2, 3, 4) representing $p < 0.05$, 0.01, 0.001, and 0.0001, respectively. Color images are available online.

did so. This is an alarming finding, given that the slope of stress/strain curves from ramp testing increases with strain magnitude, creating potentially artificially higher values. Physiologically, healthy knee cartilage typically experiences average strains under 10%,[24] and peak strains of 17%.[25] Thus, testing and quantification of the tangent modulus above these strain levels may not be clinically relevant.

To further explore and demonstrate the effect of strain and loading rate, cartilage and agarose plugs (8-mm diameter) were tested in unconfined compression at 0.1%, 1.0%, and 10.0% strain per second to a maximum of 30% strain. Plugs were allowed >1 h of rehydration in phosphate-buffered saline before retesting. No observable differences in height were present for retested samples. The resulting stress/strain relationships were analyzed by finding the slope of the curve at strains ranging from 5% to 30% (tangent modulus; Fig. 3B). For both cartilage tissue (Fig. 3F) and agarose constructs (Fig. 3G), the calculated tangent modulus increased with both strain rate and strain at calculation, indicating that these two variables should be selected carefully and kept consistent. Furthermore, testing at higher strain rates is dominated by initial fluid pressurization of cartilage tissue/constructs,[26] whereas slower strain rates (e.g., 0.1%/s) allow for some stress dissipation by fluid flow, and thus underestimate moduli that are experienced at more rapid physiological strain rates. The most common strain rate and maximum strain appear to be 1%/s and 20%, respectively, and represent a midpoint of the ranges for both parameters. Thus, *in vitro* evaluation of constructs are well accepted and may be sufficient with these test conditions.

Stress relaxation testing

Our systematic review showed that stress relaxation testing was performed almost as frequently as ramp testing. This mode of testing, outlined in Figure 4A, involves the application of a step strain (e.g., 20%), and holding said strain constant for a period of time. These tests can also involve a series of strains and relaxations (Fig. 4A, left—blue line), a so-called multistep stress-relaxation test. Ultimately, the stress response is measured, and the equilibrium stress (at the end of each relaxation period) is recorded. Finally, equilibrium modulus can be calculated by simply dividing the equilibrium stress by the equilibrium strain (mostly for one-step tests), or plotting the equilibrium stress versus strain for each step, and finding the slope of the best-fit line (Fig. 4A, right). With these fundamentals of stress relaxation testing as a basis, we found that three major parameters were most commonly provided in the literature, each of which can impact testing and analysis: strain at final step, number of steps, and relaxation time.

Upon systematic review of the stress relaxation studies, we found that the majority of studies (33/62; 53.2%) utilized between 15% and 20% as the final strain during testing (Fig. 4B). As far as the number of steps (Fig. 4C), one-step and four-step protocols were utilized in 54.8% (34/62) and 24.2% (15/62) of studies, by far the two most common step numbers used. Finally, relaxation time was highly variable, with a median of 1200 s. However, longer step durations with multistep procedures can be very time consuming.

To test whether the number of steps influences results, cartilage tissue and agarose constructs (8 mm-diameter) were tested in unconfined compression, by first applying one step of 20% strain and subsequent relaxation of 600 s. After rehydration for at least 60 min, plugs were subjected to four steps of 5% strain, with 600 s of relaxation per step. While no differences in equilibrium modulus were noted between one-step and four-step testing of cartilage (Fig. 4D; $p = 0.1289$), one-step testing appeared to overestimate the equilibrium modulus of agarose constructs compared with four-step testing (Fig. 4E; $p = 0.0073$) by about 10%. This error may be attributed to the agarose constructs not fully relaxing over the 600-s period. To explore this discrepancy, the relaxation profiles of one-step curves were fit with a one-phase decay curve, and the derivative of the curve was used to find the relaxation time required to observe a load change of <0.0001 N/min (sensitivity of Instron testing machine). The relaxation profiles of cartilage and agarose (Fig. 4F) clearly show that while cartilage profiles plateau by 600 s that agarose continues to relax. In fact, the estimated relaxation time required for agarose constructs (1161 ± 111 s) was more than double that of cartilage tissue (521 ± 233 s) in this testing configuration. Thus, careful consideration must be given to the relaxation time, depending on what type of tissue or construct is being characterized.

Creep testing

Of the compression protocols, the least commonly performed is creep testing. Creep evaluation involves the application of a constant load as the sample continues to deform, eventually reaching equilibrium (Fig. 2A, right). Unlike ramp and stress relaxation testing, creep testing is rarely performed in an unconfined configuration. The two primary parameters given for creep testing are the creep load applied and the time allowed to reach equilibrium. Due to variations in sample diameter in confined scenarios and probe diameter for *in situ* testing, comparisons were made by approximating stress from load and diameter values. Overall, the creep stress (Fig. 5A) was variable (range: 8.9–440.6 kPa) with an average of 100.2 kPa (median: 57.74 kPa). Furthermore, while creep time (Fig. 5B) was also variable (range: 300–36,000 s), the mode of 3600 s (1 h) was present in 6/15 studies (40%) that reported a duration.

To evaluate samples with a creep protocol, cartilage plugs (8 mm-diameter) were glued to a flat rigid surface and hydrated. A rigid spherical indenter (1 mm-radius) was used to apply $\sim$100 kPa of stress (0.314 N) for 3600 s. The resulting strain versus time graph, plotted in Figure 5C, demonstrates an initial asymptotic deformation, followed by apparent equilibrium soon thereafter. These data were analyzed with two methods; the first involves dividing the equilibrium stress (100 kPa) by the measured equilibrium strain to find an equilibrium modulus. However, of the 20 occurrences of creep testing, only 2 simply presented the equilibrium strain. Since creep testing is mostly performed to parse out the viscoelastic properties of a tissue (both an aggregate modulus and a permeability), many groups perform a regression analysis utilizing a poroelastic model, typically a linear biphasic model.[27–29] In fact, 75% (15/20) of the creep studies employed such an approach. For this reason, validation data obtained from testing cartilage plugs were analyzed with not only the simple equilibrium approach (as is typically done in stress relaxation testing), but also with both a Hertzian creep

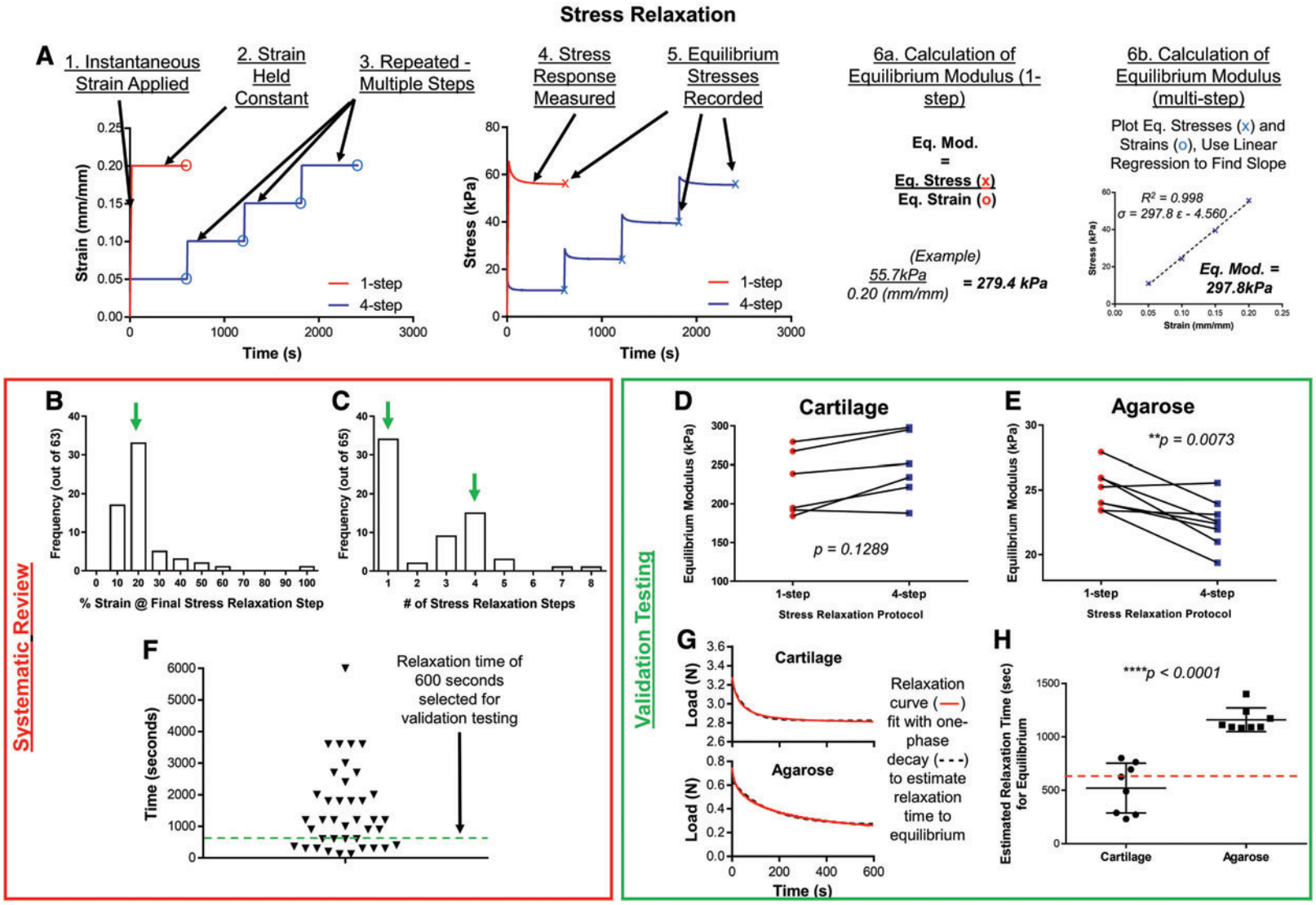

FIG. 4. Stress relaxation testing. **(A)** General methodology of stress relaxation testing, from instantaneous strain application to calculation of equilibrium modulus. Systematic review of **(B)** % strain at final relaxation step, **(C)** the number of relaxation steps, and **(F)** the time of relaxation per step. *Green arrows* and *dashed lines* represent values used for validation testing. Testing of **(D)** cartilage tissue and **(E)** agarose constructs with both one-step and four-step protocols. **(G)** Sample relaxation curves for cartilage tissue and agarose constructs were used to calculate **(H)** an estimate time for equilibrium relaxation. Color images are available online.

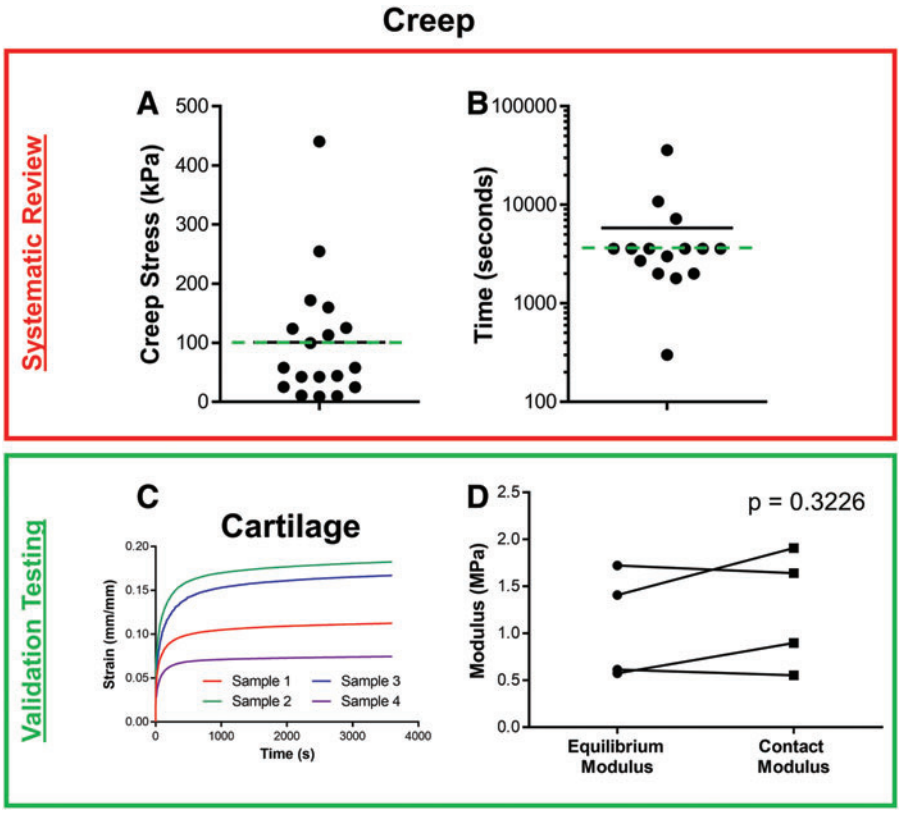

FIG. 5. Creep testing. Systematic review of **(A)** creep stress and **(B)** creep relaxation time (logarithmic scale). Mean presented with *black line*, and values used for validation testing presented with *green dashed line*. **(C)** Four cartilage samples showing creep response (strain in mm/mm) with time after application of a stress of 100 kPa. **(D)** Calculated equilibrium modulus, contact modulus, and aggregate modulus of cartilage tissues from creep testing. Color images are available online.

contact equation for spherical indentation[30,31] (Fig. 5D). While these two analysis methods show some differences between measures, these were not significant ($p=0.3226$). Biphasic theory can also be valuable in characterizing the complex mechanical properties of the tissue. For example, in addition to the aggregate moduli found in the validation testing, an average hydraulic permeability of $4.48\pm2.77\times10^{-4}$ mm^4/N×s was determined, consistent with the literature.[31] While theory is not presented in this study, many articles have derived and discussed the formulae used in such analyses.[4,29]

One consideration for creep testing, especially of tissue-engineered constructs exposed to physiological loads, is that a large deformation may occur with testing. These deformations are typically above 20% and can even exceed 50%,[32,33] resulting in significant changes to the compositional characteristics of constructs. For example, a 50% strain on a 3% agarose hydrogel in a confined setting effectively doubles the concentration of these gels to 6%. Thus, physiologic creep loading of immature constructs may be limited to lower loads to avoid these compositional changes.

Dynamic testing

The final mode of compressive testing, dynamic testing, is often applied at the end of a stress relaxation test, after the tissue has reached equilibrium. In this test, the strain is applied in a cyclic fashion while measuring the stress response (Fig. 6A), or *vice versa*. The peak-to-trough difference in stress is then divided by the peak-to-trough difference in strain to calculate a dynamic modulus (Fig. 6B). Other dynamic properties commonly calculated are energy dissipation, hysteresis, and phase lag. The typical input parameters for dynamic testing are cycle frequency, the number of cycles, and the strain amplitude. Our literature review of dynamic testing showed that frequency ranged from 0.01 to 100 Hz, but was most commonly set to either 0.1 or 1.0 Hz (Fig. 6C, red lines). As for the number of cycles (Fig. 6D), there was an even greater range, between 5 and 100,000 cycles, and the geometric mean of the number of cycles was 109.3 cycles. The studies at the higher end of this range typically characterize a tissue or construct's long-term mechanical behavior,[34] transitioning from simple compaction to fatigue resistance.[35] Finally, a range of strain amplitudes were used, given in terms of strain (e.g., 1%) or deformation (e.g., 50 μm). Of the 16 studies that reported the amplitude as a strain (Fig. 6E), the mode of 1% strain amplitude was utilized 7 times.

To illustrate test sample response to dynamic conditions, agarose gels (8-mm diameter) were compressed to 10% strain, relaxed for 600 s, and subjected to cyclic strain. Specifically, gels were compressed with 1% strain amplitude for 100 cycles, either at 0.1 or 1.0 Hz. Furthermore, during analysis, either the first 10 or 100 cycles were analyzed to calculate dynamic modulus. Frequency impacted the calculated dynamic modulus ($p=0.0003$), whereas the number of cycles for analysis did not ($p=0.1030$), with testing at 1.0 Hz giving a modulus 8.2–33.6% greater than testing at 0.1 Hz (Fig. 6F). For this reason, many studies test at multiple frequencies, sometimes as part of a frequency sweep, elucidating viscoelastic properties.[36–39]

A final consideration for dynamic cartilage testing involves frequencies that are too high, causing the platen to separate from the sample and creating ''squared'' regions of the data that make it difficult to assess true tissue properties. These regions can be identified and quantified by measuring

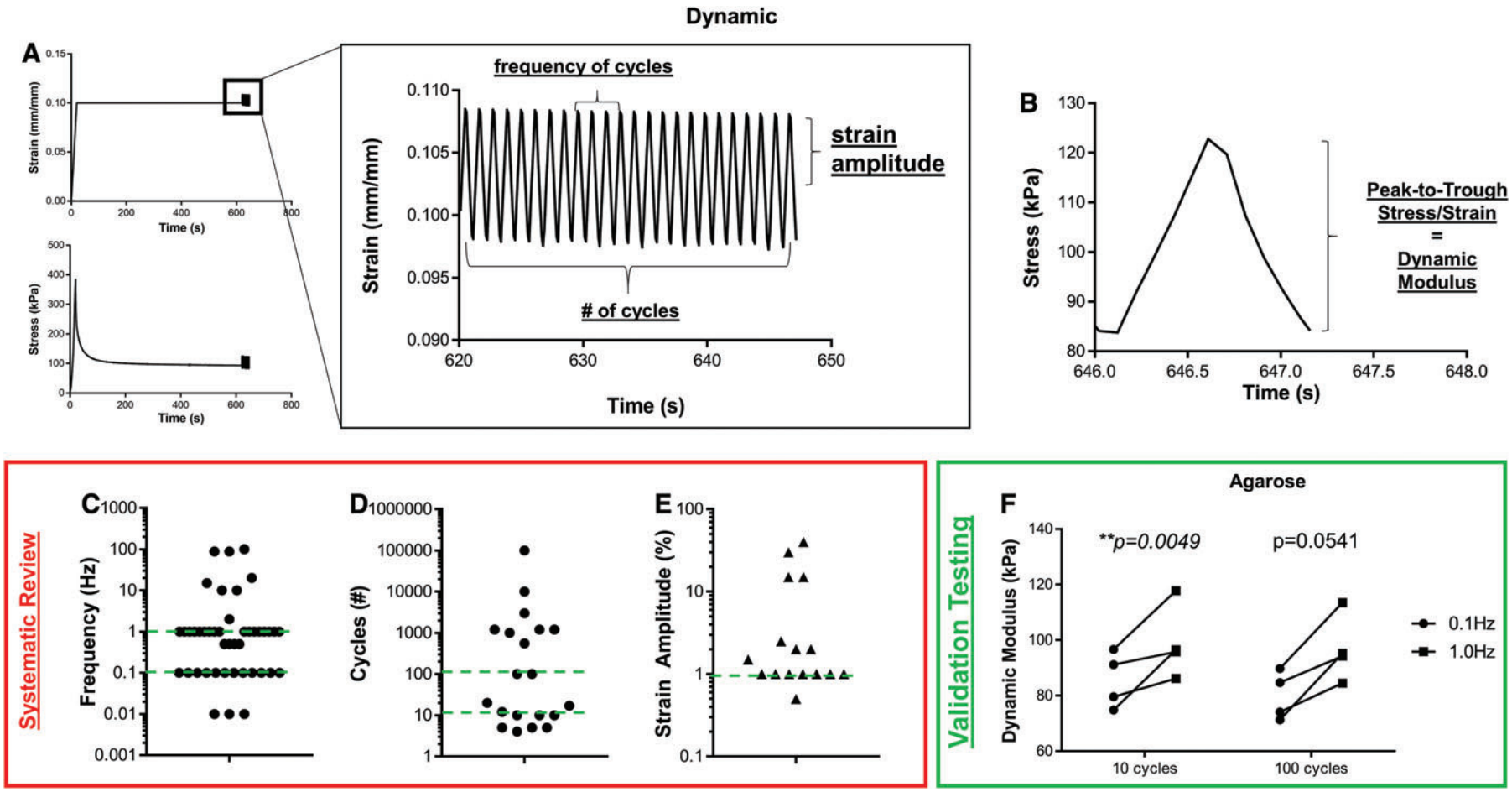

FIG. 6. Dynamic testing. **(A)** Samples are typically subjected to a specified strain, allowed to relax until equilibrium, and then cyclically compressed at a specified frequency, number of cycles, and strain amplitude. The corresponding stress response is then used to calculate **(B)** dynamic modulus, the peak-to-trough stress divided by strain. Systematic review of **(C)** frequency, **(D)** number of cycles, and **(E)** strain amplitude show high variability among studies. *Green dashed lines* represent testing parameters chosen for validation studies. **(F)** Validation testing of agarose gels determined that dynamic frequency impacts calculated dynamic modulus. Color images are available online.

the harmonic distortion of loading, whether by observing deformities in the loading waveform,[38] or performing a Fourier analysis to identify nonlinearity.[40] Mauck *et al.*[41] found that at a dynamic frequency of 1 Hz, strain amplitudes of >10% prevented lift-off from engineered chondrocyte-seeded agarose constructs. However, with the variety of dynamic frequencies and amplitudes, as well as differential responses between tissues and constructs, verification of harmonic loading should be performed for each application.

Considerations for testing configuration

Testing configuration can certainly have an impact on results.[42] Perhaps the simplest of the configurations is unconfined compression, which only involves two flat platens, with the sample placed between. Users should verify that the platens are parallel, and that the two surfaces of the testing sample are parallel, to avoid malalignment. Malalignment can cause the platen to make contact with only a portion of the sample face, decreasing the stress applied and leading to underestimation of properties.

Confined testing requires either a porous indenter or a porous base to allow for unidirectional fluid flow. While not an overly complicated configuration, confined compression testing is more complicated than unconfined testing, especially with regard to the viscoelastic modeling that typically accompanies it.[29,43,44] For confined testing, it is crucial that the indenter does not contact the side walls of the confined chamber, as this will register false load readings. Additionally, the porosity and stiffness of the indenter can lead to a interdigitating contact between the platen and tissue/construct. For softer constructs and hydrogels, expansion of sample materials into the pores of the platen may occur; incorporation of this interdigitation into analysis may be necessary for accurate estimation of material properties.[45] Furthermore, the assumption of frictionless versus perfectly adhesive contact between platen and tissue/construct should be considered as it has implications on viscoelastic modeling solutions,[46,47] both in unconfined[48] and confined[49] compression.

Finally, *in situ* testing relies upon embedding the sample in a rigid assembly, either an entire osteochondral segment for cartilage tissue, or a construct larger than the probe used for testing. A flat-ended cylindrical or spherical indenter probe is then used to apply stress or strain to the tissue/construct. For all configurations of compression testing, rigid connectors are required, as any laxity can lead to abrupt changes in either strain or stress.

A final consideration to testing samples in compression is the size of samples and probes used (Fig. 7). Of the 103 unconfined protocols and 20 confined protocols, only 3 occurrences of noncircular cross-sections were observed, meaning that groups typically test cylindrical constructs. A review of all compression protocols showed that unconfined and confined testing typically used average sample diameters of 5.46 ± 1.85 and 4.85 ± 1.25 mm, respectively. Sample height can also have an impact on outcomes, especially as it relates to the diameter. Typically, samples with a width/height aspect ratio of at least 2 (twice as wide as high) should be utilized to avoid sample buckling into a ''parallelogram'' deformation. With regard to *in situ* testing, of the 54 occurrences, 11 used spherical probes and 27 used cylindrical (flat-ended) probes, with an additional 16 unspecified geometries.

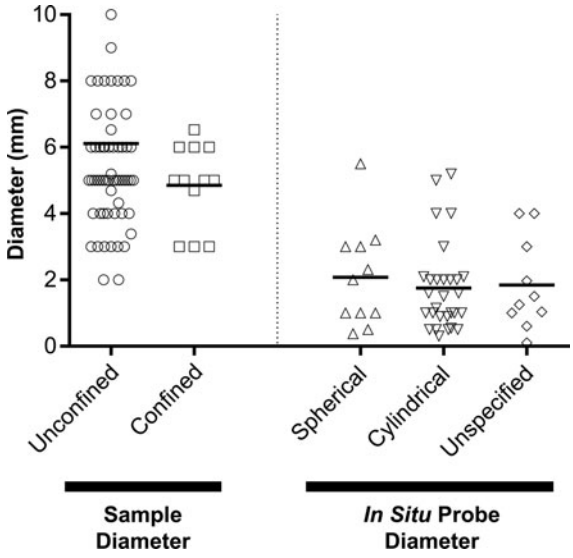

FIG. 7. Sample diameters (for unconfined and confined compression) and probe diameters (for *in situ* testing) from systematic review.

The average probe diameter of all indentation probes was 1.84 mm, notably less than the unconfined and confined sample diameters, indicating smaller contact geometries with *in situ* configurations. Of note, the tissue or construct diameter needs to be greater than the probe diameter to assure full contact between the probe and sample. For example, Meloni *et al.*[50] determined, through finite element modeling that when testing with a 2-mm-diameter spherical indenter, a diameter of at least 6 mm was required to accurately measure reaction forces and fluid pressurization. Thus, the size and geometry of both samples and probes should be considered, especially as it relates to outcome values.

Alternative Testing Types

While compression is by far the most common type of testing, other techniques are very important to physically evaluate the efficacy of a treatment. For example, studies aimed at improving cartilage tribology are interested in determining the lubrication modes and coefficient of friction at the articulating surface. Furthermore, other techniques probe the micromechanics of the cartilage tissue, as well as the integration between constructs and the surrounding tissue. The following section provides a brief description of these testing methods, utilizing the studies from the systematic review.

Lubrication

Maintaining a low friction interface is essential for tissue longevity due to the load-bearing nature where cartilage experiences millions of sliding cycles per year. It is well understood that elevated friction in a synovial joint can lead to both mechanical wear and erosion of the articular surface[51,52] in addition to instigating adverse biological responses in chondrocytes such as apoptosis.[53,54] With this in mind, lubrication of engineered or repair tissue is not only important to ensure its own longevity, but also the homeostasis of the contacting cartilage it will articulate against. Consequently, there has been recent emphasis in promoting effective lubrication of engineered or repaired cartilage tissue.

Healthy articular cartilage relies on a combination of lubricating mechanisms, where the structure of articular cartilage and biomolecular makeup of the articular surface both serve to reduce friction to provide a well lubricated interface.[55–57] First, the structure of articular cartilage, specifically its low hydraulic permeability, causes the articular surface to be supported by high interstitial fluid pressures by the same mechanism that causes strain rate-dependent stiffening of cartilage described above.[55,58,59] In essence, there is a load sharing between the solid (Fig. 8, P_s) and fluid states (P_f) at the articular surface. The higher the proportion of load supported by fluid pressurization, the lower the friction coefficient at the articular surface will be. The other mechanism of lubrication for articular cartilage depends on surface chemistry and lubricating biomolecules, such as lubricin and hyaluronic acid.[60] These two molecules interact with the articular surface and reduce friction through a mechanism called boundary lubrication.[56,57]

Due to the relative contributions of these two mechanisms in cartilage lubrication, two main methods for testing cartilage lubrication properties have emerged (Fig. 8). The first method uses a migrating contact area (Fig. 8A).[58,61] In this testing mode, a probe migrates across the cartilage surface causing dynamic deformation in the cartilage matrix. Consequently, friction coefficients are typically very low in this testing configuration as fluid pressure (P_f) is maintained by the active deformation of the cartilage surface. This load support can be described by the Peclet number, where low friction occurs when Pe >> 1 and convective fluid velocity surpasses diffusive fluid velocity.[55,61] Simply put, this testing configuration is robust in measuring the fluid pressurization potential of native and engineered cartilage. This response is sensitive to cartilage mechanical properties described above, such as the compressive and tensile moduli and the hydraulic permeability.[62]

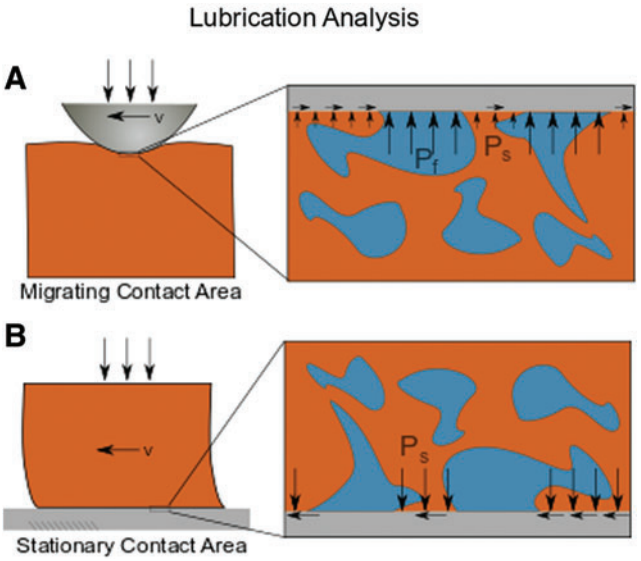

FIG. 8. Lubrication. Schematics of the two major forms of lubrication analysis are **(A)** migrating contact area and **(B)** stationary contact area. Depictions of stresses on the solid phase (P_s) and fluid phase (P_f) for each analysis are shown. Color images are available online.

The second method of lubrication analysis uses a stationary contact area configuration and is designed to be more sensitive to boundary lubrication (Fig. 8B). In this method, a sample is compressed against a rigid counterface (e.g., glass slide, polished stainless steel), and the friction coefficient is tracked over time as interstitial fluid pressure drops to the ambient pressure.[61,63] Once interstitial fluid pressure subsides and the normal load is supported by solid/solid contact ($P_s > 0$, $P_f \approx 0$), the friction coefficient is dictated by the structural and biochemical makeup of the articular surface. Consequently, this testing configuration is sensitive to factors such as lubricin localization to the articular surface or interactions with other lubricating biomolecules such as hyaluronic acid.

Because these two methods to measure friction coefficients provide different information about the lubricating ability of both native and engineered cartilage, special care is necessary when interpreting results. For example, a tissue surface that promotes localization of lubricants, but has a high permeability would have a relatively low friction coefficient in a stationary contact area experiment compared with a relatively high coefficient of friction in a migrating contact area experiment. Conversely, a tissue that is effective at pressurizing interstitial fluid but fails to boundary lubricate effectively would have a relatively low friction coefficient in a migrating contact area experiment, but a relatively high friction coefficient in a stationary contact area experiment. Consequently, it is difficult to understand the true lubricating ability of a tissue and compare between studies that utilize different testing methods without taking both mechanisms of lubrication into account.

Nanoindentation

Similar to lubrication, nanoindentation has emerged recently as a metric used to understand the complex mechanics of healthy and engineered cartilage tissues at lower length scales. Often, nanoindentation is conducted using an atomic force microscope equipped with colloidal or pyramidal tips that can probe the cartilage surface with high spatial resolution.[64] Often working under the assumption that the Peclet number is low (see Lubrication section), the force displacement curves are fit to a model, such as a modified Hertzian contact model for colloidal probes,[65] to extract parameters such as the local indentation modulus. The size of tips can be highly variable (systematic review: 10 nm–100 μm) to elucidate individual matrix fiber properties, as well as overall microscale tissue properties. Recent advances in this technique have focused on understanding the heterogeneity of cartilage and engineered tissue both in terms of spatial variation in moduli as well as stiffness gradients between the ECM, the pericellular matrix, and the chondrocytes.[66,67] Indeed, testing is trending toward microscopic systems,[54,67] enabling the determination of localized properties in both developing and regenerating tissues.

Other testing

Additional testing modes of cartilage tissues and constructs include tensile, shear, and integration testing. Articular cartilage is robust at supporting tensile stresses in the superficial zone, as aligned superficial bundles resist stresses parallel to the articulating surface. However, only a limited

number of studies during the review period tested the tensile properties of the superficial zone of cartilage[68,69]; from this systematic review, tensile testing was typically performed on scaffolds/constructs developed for cartilage tissue engineering (20/23; 87.0%). Scaffolds were typically cut into either rectangular or dogbone-shaped samples,[70,71] yet no consistent loading profiles and rates were observed. These properties are certainly integral to those aiming to create the cartilage superficial zone, and comparison to native tissue can help normalize studies with different loading schemes. Tensile properties also contribute substantially to the effective compressive modulus when evaluated by indentation or in unconfined compression,[70,72] where the Poisson's ratio of cartilage is often quite low and depends on the tensile properties of the specimen.[73,74]

The final two forms of testing, shear and integration, were performed by <2% of all studies that were systematically reviewed. Shear testing has been used for a variety of purposes, including but not limited to characterization of the cartilage/bone interface,[75] tissue/scaffold interface,[76] transitional zone shear properties,[77] and torsional resistance.[78] Depth-dependent shear properties can also be quantified, through microscope-guided strain mapping, where compressive and shear loads are applied to tissue or construct hemicylinders.[79] By matrix staining with DAPI to identify nuclei or 5-dichlorotriazinyl-aminofluorescein to image matrix, local shear strains and moduli in the tissue can be calculated, for native tissue[80] and constructs.[81]

Integration testing, on the other hand, typically involves testing the physical joining of constructs to surrounding articular cartilage that occurs through biological remodeling, either by push-out, lap-shear, or uniaxial tension testing. In the push-out scenario, used for testing cartilage or meniscus integration, a cylindrical punch is cored and replaced by a scaffold or construct and cultured for a duration of time to strengthen the interface.[82–85] The inner core is then pushed out of the outer core with an indenter, allowing for calculation of the integration strength. Another method for testing cartilage integration approaches involves lap-shear testing,[86–88] which is achieved by fixing each side of an interface to a substrate or clamping, and applying tension parallel to the adhesive interface. Finally, cartilage integration is often tested in uniaxial tension. For example, in culture or subcutaneous rodent models a scaffold can be placed between two cartilage discs, after which integration is evaluated by applying tension to the two cartilage discs.[89,90] These forms of testing are extremely valuable to groups attempting to improve on the typically poor integration of cartilage constructs.

Guidance Documents and Potential Standardization

Mechanical characterization of repaired or regenerate articular cartilage is vital for its translation and, ultimately, clinical use. To aid in this translation, the United States Food and Drug Administration (FDA) and International Cartilage Repair Society (ICRS) have published guidance documents[91,92] with recommendations for preclinical study outcomes of cartilage repair, each containing a section on mechanical testing outcomes. These two documents focus on compression as a primary mode of testing, with mention of biphasic or poroelastic modeling to determine viscoelastic properties (aggregate modulus, permeability). Interestingly, the ASTM standard on cartilage repair and regeneration (F2451-05[93]) only describes confined creep testing as a requirement for mechanical evaluation, and suggests that creep indentation curves should be fit to Mow's biphasic theory[4] to obtain aggregate modulus and permeability.

The FDA and ICRS documents both recommend expanding on this to carry out dynamic testing to quantify the physiological response, in addition to the aforementioned static (creep or stress relaxation) testing to quantify material properties. From our systematic review, of the 158 studies to perform compression testing, only 18 (11.4%) performed both static time-dependent tests (stress relaxation, creep) and dynamic testing, indicating that the majority of these studies did not satisfy the recommendations of the FDA and ICRS guidance documents. The FDA and ICRS documents are also more flexible with regard to configuration, indicating that unconfined, confined, and indentation configurations are all adequate. Furthermore, the FDA and ICRS documents allude to other testing types (shear, integration, tension, lubrication, wear; Table 1) as being important, but do not provide an accompanying description. Certainly, these properties are integral to the function evaluation of cartilage therapies, and should be evaluated in addition to compression testing. Of the 197 studies included in the systematic review, 158 performed one testing type, 30 performed two, 5 performed three, and only 2 studies performed four types of testing. These two studies[94,95] performed a comprehensive battery of tests, and serve as examples of multifunctional evaluation of cartilage constructs.

Even with these guidance documents, only ~25% of studies since 2011 (publishing of documents) adhered to the mechanical testing set forth in these documents.[96] Thus, if novel replacement and therapeutics are aiming for clinical translation, better adherence to these documents will be required, and will need to include multiple mechanical evaluations (static and dynamic compression, lubrication, integration, wear). That being said, none of the three documents (FDA, ICRS, ATSM) gives suggestions on specific test parameters and rates. While physiological loading is

Table 1. Guidance Documents

	FDA	*ICRS*	*ASTM*
Testing type			
Compression	x	x	x
Lubrication/Friction		x	
Shear	x		
Tension	x	x	
Integration/Fixation	x		
Wear	x	x	
Fatigue		x	
Mode			
Quasistatic	x	x	x
Dynamic	x	x	
Configuration			
Unconfined	x	x	
Confined	x	x	x
Indentation	x	x	

Testing types, modes, and configurations suggested by the Food and Drug Administration (FDA[91]), the International Cartilage Repair Society (ICRS[92]), and the American Society for Testing and Materials (ASTM[93]).

recommended, standardization of testing protocols would be greatly beneficial to cartilage tissue engineers. Our recommendations on testing parameters and protocols, derived from our analysis and consideration of both clinical/functional relevance and common procedures, are provided below:

1. Time-Dependent Compression Testing (at least one)
   a. Stress relaxation (four steps of 5% strain; >10-min relaxation)
   b. Creep (100 kPa for constructs, 1 MPa for cartilage; >60-min relaxation)
2. Dynamic Compression Testing
   a. Following 10–20% stress relaxation
   b. One to 10% strain amplitude at 1 Hz for >10 cycles
3. Other Testing (dependent upon application)
   a. Lubrication (required for viscosupplementation and superficial cartilage studies)
   b. Nanoindentation (for microscopic mapping/characterization of pericellular matrix/ECM properties)
   c. Shear (highly recommended for all studies)
   d. Integration (to assess lateral integration)
4. Testing configurations
   a. Unconfined or confined for constructs
   b. Indentation for explants (to preserve the osteochondral unit)

Conclusions and Future Directions

Articular cartilage is an organizationally and compositionally complex tissue, allowing it to withstand an array of dynamic stresses of high magnitude that arise with the activities of daily living. The inherent properties of cartilage aid in this resistance, but are compromised and can progressively deteriorate after injury or with disease. Novel treatments and scaffolds are constantly being developed, and the mechanical function of the cartilage tissue or regenerating construct is paramount for its efficacy. This study systematically reviewed the articular cartilage mechanical testing literature from the last 10 years, showing that the majority of studies performed compression testing. Further exploration of modes, configurations, and testing parameters revealed high variability in test criteria and analysis methods, motivating the standardization of these approaches. Validation testing of many of these key parameters demonstrated their influence on outcome measures. Thus, careful consideration to testing protocols and method of analysis must be taken, and this work serves as a guide for those undertaking such studies. Standardization of testing and reporting measures will enable more ready comparison between studies, and this will undoubtedly speed development of these constructs.

Many of the testing configurations and techniques mentioned throughout this review have been utilized for decades, mostly to evaluate harvested cartilage specimens from animal studies, constructs from *in vitro* culture studies, and scaffolds from fabrication studies. Techniques to evaluate *in vivo* cartilage mechanics have also been developed, and even utilized clinically. For example, Lyyra *et al.*[97] developed an arthroscopically applicable device to indent cartilage; these indentation devices can characterize the health of living cartilage and identify functional changes that may not be visually apparent through arthroscopy and imaging modalities. These techniques have since been modified to apply dynamic loads that further quantify stiffness,[98,99] providing further insight into early cartilage degeneration. As these physical technologies have progressed with time, imaging modalities have also advanced to the point that mechanical deformations can be determined *in vivo* with high spatial resolution. Both magnetic resonance imaging[24] and ultrasound elastography[100] can be used in preclinical and clinical studies to noninvasively and nondestructively predict mechanical properties,[101–103] a potential future of the field. Moreover, the ability to perform these analyses at nonterminal time points allows for the ability to evaluate the mechanical maturation of cartilage constructs or protective capabilities of therapeutics. Certainly, while these novel approaches are on the horizon, cartilage tissue engineers stand to benefit from a detailed review and validation of current cartilage mechanical testing techniques.

Acknowledgments

This work was supported by the Penn Center for Musculoskeletal Disorders Biomechanics Core (P30 AR069619), the National Institutes of Health (R01 EB008722, R01 AR071340, R01 AR056145, F32 AR072478), and the Department of Veterans Affairs (RX00700).

Disclosure Statement

No competing financial interests exist. R.L.M. is coeditor-in-chief of the *Journal of Orthopedic Research, Spine*.

Supplementary Material

Supplementary Table S1

References

1. Sophia Fox, A.J., Bedi, A., and Rodeo, S.A. The basic science of articular cartilage: structure, composition, and function. Sports Health **1,** 461, 2009.
2. Wang, H.A., and Ateshian, G. The normal stress effect and equilibrium friction coefficient of articular cartilage under steady frictional shear. J Biomech **30,** 771, 1997.
3. Korhonen, R.K., Julkunen, P., Wilson, W., and Herzog, W. Importance of collagen orientation and depth-dependent fixed charge densities of cartilage on mechanical behavior of chondrocytes. J Biomech Eng **130,** 21003, 2008.
4. Mow, V.C., Kuei, S.C., Lai, W.M., and Armstrong, C.G. Biphasic creep and stress relaxation of articular cartilage in compression: theory and experiments. J Biomech Eng **102,** 73, 1980.
5. Bartell, L.R., Fortier, L.A., Bonassar, L.J., and Cohen, I. Measuring microscale strain fields in articular cartilage during rapid impact reveals thresholds for chondrocyte death and a protective role for the superficial layer. J Biomech **48,** 3440, 2015.
6. Zevenbergen, L., Smith, C.R., Van Rossom, S., *et al.* Cartilage defect location and stiffness predispose the tibiofemoral joint to aberrant loading conditions during stance phase of gait. PLoS One **13,** e0205842, 2018.
7. Gomoll, A.H., and Minas, T. The quality of healing: articular cartilage. Wound Repair Regen **22(Suppl 1),** 30-8, 2014.
8. Asik, M., Ciftci, F., Sen, C., Erdil, M., and Atalar, A. The microfracture technique for the treatment of full-thickness

articular cartilage lesions of the knee: midterm results. Arthrosc J Arthrosc Relat Surg **24,** 1214, 2008.
9. Kreuz, P.C., Steinwachs, M.R., Erggelet, C., *et al.* Results after microfracture of full-thickness chondral defects in different compartments in the knee. Osteoarthritis Cartilage **14,** 1119, 2006.
10. Harris, J.D., Siston, R.A., Pan, X., and Flanigan, D.C. Autologous chondrocyte implantation. J Bone Joint Surg Am **92,** 2220, 2010.
11. Peterson, L., Vasiliadis, H.S., Brittberg, M., and Lindahl, A. Autologous chondrocyte implantation: a long-term follow-up. Am J Sports Med **38,** 1117, 2010.
12. Benthien, J.P., and Behrens, P. Autologous matrix-induced chondrogenesis (AMIC): combining microfracturing and a collagen I/III matrix for articular cartilage resurfacing. Cartilage **1,** 65, 2010.
13. Solheim, E., Hegna, J., Inderhaug, E., Øyen, J., Harlem, T., and Strand, T. Results at 10–14 years after microfracture treatment of articular cartilage defects in the knee. Knee Surg Sport Traumatol Arthrosc **24,** 1587, 2016.
14. Patel, J.M., Saleh, K.S., Burdick, J.A., and Mauck, R.L. Bioactive factors for cartilage repair and regeneration: improving delivery, retention, and activity. Acta Biomater **93,** 222, 2019.
15. Dickinson, S.C., Sims, T.J., Pittarello, L., Soranzo, C., Pavesio, A., and Hollander, A.P. Quantitative outcome measures of cartilage repair in patients treated by tissue engineering. Tissue Eng **11,** 277, 2005.
16. Hoemann, C., Kandel, R., Roberts, S., *et al.* International Cartilage Repair Society (ICRS) recommended guidelines for histological endpoints for cartilage repair studies in animal models and clinical trials. Cartilage **2,** 153, 2011.
17. Olvera, D., Daly, A., and Kelly, D.J. Mechanical testing of cartilage constructs. Methods Mol Biol **1340,** 279, 2015.
18. Xiao, Y., Friis, E.A., Gehrke, S.H., and Detamore, M.S. Mechanical testing of hydrogels in cartilage tissue engineering: beyond the compressive modulus. Tissue Eng Part B Rev **19,** 403, 2013.
19. Lakin, B.A., Snyder, B.D., and Grinstaff, M.W. Assessing cartilage biomechanical properties: techniques for evaluating the functional performance of cartilage in health and disease. Annu Rev Biomed Eng **19,** 27, 2017.
20. Mow, V.C., Holmes, M.H., and Michael Lai, W. Fluid transport and mechanical properties of articular cartilage: a review. J Biomech **17,** 377, 1984.
21. Quiroga, J.M.P., Wilson, W., Ito, K., and van Donkelaar, C.C. Relative contribution of articular cartilage's constitutive components to load support depending on strain rate. Biomech Model Mechanobiol **16,** 151, 2017.
22. Rodriguez, M.L., and Li, L. Compression-rate-dependent nonlinear mechanics of normal and impaired porcine knee joints. BMC Musculoskelet Disord **18,** 447, 2017.
23. Park, S., Krishnan, R., Nicoll, S.B., and Ateshian, G.A. Cartilage interstitial fluid load support in unconfined compression. J Biomech **36,** 1785, 2003.
24. Chan, D.D., Cai, L., Butz, K.D., Trippel, S.B., Nauman, E.A., and Neu, C.P. In vivo articular cartilage deformation: noninvasive quantification of intratissue strain during joint contact in the human knee. Sci Rep **6,** 19220, 2016.
25. Carter, T.E., Taylor, K.A., Spritzer, C.E., *et al.* In vivo cartilage strain increases following medial meniscal tear and correlates with synovial fluid matrix metalloproteinase activity. J Biomech **48,** 1461, 2015.
26. Li, L.P., and Herzog, W. Strain-rate dependence of cartilage stiffness in unconfined compression: the role of fibril reinforcement versus tissue volume change in fluid pressurization. J Biomech **37,** 375, 2004.
27. Mak, A.F., Lai, W.M., and Mow, V.C. Biphasic indentation of articular cartilage-I. Theoretical analysis. J Biomech **20,** 703, 1987.
28. Mow, V.C., Gibbs, M.C., Lai, W.M., Zhu, W.B., and Athanasiou, K.A. Biphasic indentation of articular cartilage-II. A numerical algorithm and an experimental study. J Biomech **22,** 853, 1989.
29. Soltz, M.A., and Ateshian, G.A. Experimental verification and theoretical prediction of cartilage interstitial fluid pressurization at an impermeable contact interface in confined compression. J Biomech **31,** 927, 1998.
30. Desrochers, J., Amrein, M.W., and Matyas, J.R. Viscoelasticity of the articular cartilage surface in early osteoarthritis. Osteoarthritis Cartilage **20,** 413, 2012.
31. Moore, A.C., DeLucca, J.F., Elliott, D.M., and Burris, D.L. Quantifying cartilage contact modulus, tension modulus, and permeability with Hertzian biphasic creep. J Tribol **138,** 414051, 2016.
32. Thambyah, A., van Heeswijk, V.M., van Donkelaar, C.C., and Broom, N. A microstructural study of load distribution in cartilage: a comparison of stress relaxation versus creep loading. Adv Mater Sci Eng **2015,** 11, 2015.
33. Charlton, D.C., Peterson, M.G.E., Spiller, K., Lowman, A., Torzilli, P.A., and Maher, S.A. Semi-degradable scaffold for articular cartilage replacement. Tissue Eng Part A **14,** 207, 2008.
34. Vikingsson, L., Gómez-Tejedor, J.A., Gallego Ferrer, G., and Gómez Ribelles, J.L. An experimental fatigue study of a porous scaffold for the regeneration of articular cartilage. J Biomech **48,** 1310, 2015.
35. Kaplan, J.T., Neu, C.P., Drissi, H., Emery, N.C., and Pierce, D.M. Cyclic loading of human articular cartilage: the transition from compaction to fatigue. J Mech Behav Biomed Mater **65,** 734, 2017.
36. Temple, D.K., Cederlund, A.A., Lawless, B.M., Aspden, R.M., and Espino, D.M. Viscoelastic properties of human and bovine articular cartilage: a comparison of frequency-dependent trends. BMC Musculoskelet Disord **17,** 419, 2016.
37. Suh, J.-K., Li, Z., and Woo, S.L.-Y. Dynamic behavior of a biphasic cartilage model under cyclic compressive loading. J Biomech **28,** 357, 1995.
38. Park, S., Hung, C.T., and Ateshian, G.A. Mechanical response of bovine articular cartilage under dynamic unconfined compression loading at physiological stress levels. Osteoarthritis Cartilage **12,** 65, 2004.
39. Fulcher, G.R., Hukins, D.W.L, and Shepherd, D.E.T. Viscoelastic properties of bovine articular cartilage attached to subchondral bone at high frequencies. BMC Musculoskelet. Disord **10,** 61, 2009.
40. Lee, R.C., Frank, E.H., Grodzinsky, A.J., and Roylance, D.K. Oscillatory compressional behavior of articular cartilage and its associated electromechanical properties. J Biomech Eng **103,** 280, 1981.
41. Mauck, R.L., Soltz, M.A., Wang, C.C.B., Wong, D.D., Chao, P.G., and Ateshian, G.A. Functional tissue engineering of articular cartilage through dynamic loading of chondrocyte-seeded agarose gels. J Biomech Eng **122,** 252, 2000.

42. Korhonen, R.K., Laasanen, M.S., Töyräs, J., *et al.* Comparison of the equilibrium response of articular cartilage in unconfined compression, confined compression and indentation. J Biomech **35,** 903, 2002.
43. Soltz, M.A., and Ateshian, G.A. Interstitial fluid pressurization during confined compression cyclical loading of articular cartilage. Ann Biomed Eng **28,** 150, 2000.
44. Soltz, M.A., and Ateshian, G.A. A conewise linear elasticity mixture model for the analysis of tension-compression nonlinearity in articular cartilage. J Biomech Eng **122,** 576, 2000.
45. Buschmann, M.D., Soulhat, J., Shirazi-Adl, A., Jurvelin, J.S., and Hunziker, E.B. Confined compression of articular cartilage: linearity in ramp and sinusoidal tests and the importance of interdigitation and incomplete confinement. J Biomech **31,** 171, 1997.
46. Armstrong, C.G., Lai, W.M., and Mow, V.C. An analysis of the unconfined compression of articular cartilage. J Biomech Eng **106,** 165, 1984.
47. Kim, Y.J., Bonassar, L.J., and Grodzinsky, A.J. The role of cartilage streaming potential, fluid flow and pressure in the stimulation of chondrocyte biosynthesis during dynamic compression. J Biomech **28,** 1055, 1995.
48. Spilker, R.L., Suh, J.-K., and Mow, V.C. Effects of friction on the unconfined compressive response of articular cartilage: a finite element analysis. J Biomech Eng **112,** 138, 1990.
49. Chen, A.C., Nguyen, T.T., and Sah, R.L. Streaming potentials during the confined compression creep test of normal and proteoglycan-depleted cartilage. Ann Biomed Eng **25,** 269, 1997.
50. Meloni, G.R., Fisher, M.B., Stoeckl, B.D., Dodge, G.R., and Mauck, R.L. Biphasic finite element modeling reconciles mechanical properties of tissue-engineered cartilage constructs across testing platforms. Tissue Eng Part A **23,** 663, 2017.
51. Jay, G.D., Torres, J.R., Rhee, D.K., *et al.* Association between friction and wear in diarthrodial joints lacking lubricin. Arthritis Rheum **56,** 3662, 2007.
52. Oungoulian, S.R., Durney, K.M., Jones, B.K., Ahmad, C.S., Hung, C.T., and Ateshian, G.A. Wear and damage of articular cartilage with friction against orthopedic implant materials. J Biomech **48,** 1957, 2015.
53. Waller, K.A., Zhang, L.X., Elsaid, K.A., Fleming, B.C., Warman, M.L., and Jay, G.D. Role of lubricin and boundary lubrication in the prevention of chondrocyte apoptosis. Proc Natl Acad Sci U S A **110,** 5852, 2013.
54. Bonnevie, E.D., Delco, M.L., Bartell, L.R., *et al.* Microscale frictional strains determine chondrocyte fate in loaded cartilage. J Biomech **74,** 72, 2018.
55. Ateshian, G.A. The role of interstitial fluid pressurization in articular cartilage lubrication. J Biomech **42,** 1163, 2009.
56. Schmidt, T.A., Gastelum, N.S., Nguyen, Q.T., Schumacher, B.L., and Sah, R.L. Boundary lubrication of articular cartilage: role of synovial fluid constituents. Arthritis Rheum **56,** 882, 2007.
57. Bonnevie, E.D., Galesso, D., Secchieri, C., Cohen, I., and Bonassar, L.J. Elastoviscous transitions of articular cartilage reveal a mechanism of synergy between lubricin and hyaluronic acid. PLoS One **10,** e0143415, 2015.
58. Bonnevie, E.D., Baro, V., Wang, L., and Burris, D.L. In-situ studies of cartilage microtribology: roles of speed and contact area. Tribol Lett **41,** 83, 2011.
59. Krishnan, R., Kopacz, M., and Ateshian, G.A. Experimental verification of the role of interstitial fluid pressurization in cartilage lubrication. J Orthop Res **22,** 565, 2004.
60. Gleghorn, J.P., and Bonassar, L.J. Lubrication mode analysis of articular cartilage using Stribeck surfaces. J Biomech **41,** 1910, 2008.
61. Caligaris, M., and Ateshian, G.A. Effects of sustained interstitial fluid pressurization under migrating contact area, and boundary lubrication by synovial fluid, on cartilage friction. Osteoarthritis Cartilage **16,** 1220, 2008.
62. Bonnevie, E.D., Baro, V.J., Wang, L., and Burris, D.L. Fluid load support during localized indentation of cartilage with a spherical probe. J Biomech **45,** 1036, 2012.
63. Gleghorn, J.P., Jones, A.R.C., Flannery, C.R., and Bonassar, L.J. Boundary mode lubrication of articular cartilage by recombinant human lubricin. J Orthop Res **27,** 771, 2009.
64. Plodinec, M., Loparic, M., and Aebi, U. Imaging articular cartilage tissue using atomic force microscopy (AFM). Cold Spring Harb Protoc **2010,** 2010. DOI: 10.1101/pdb.prot5499.
65. Park, S., Costa, K.D., Ateshian, G.A., and Hong, K.S. Mechanical properties of bovine articular cartilage under microscale indentation loading from atomic force microscopy. Proc Inst Mech Eng Part H J Eng Med **223,** 339, 2009.
66. Darling, E.M., Wilusz, R.E., Bolognesi, M.P., Zauscher, S., and Guilak, F. Spatial mapping of the biomechanical properties of the pericellular matrix of articular cartilage measured in situ via atomic force microscopy. Biophys J **98,** 2848, 2010.
67. Han, B., Nia, H.T., Wang, C., *et al.* AFM-Nanomechanical test: an interdisciplinary tool that links the understanding of cartilage and meniscus biomechanics, osteoarthritis degeneration, and tissue engineering. ACS Biomater Sci Eng **3,** 2033, 2017.
68. Kempson, G.E. Relationship between the tensile properties of articular cartilage from the human knee and age. Ann Rheum Dis **41,** 508, 1982.
69. Mansfield, J.C., Bell, J.S., and Winlove, C.P. The micromechanics of the superficial zone of articular cartilage. Osteoarthritis Cartilage **23,** 1806, 2015.
70. Huang, A.H., Yeger-McKeever, M., Stein, A., and Mauck, R.L. Tensile properties of engineered cartilage formed from chondrocyte- and MSC-laden hydrogels. Osteoarthritis Cartilage **16,** 1074, 2008.
71. Ahsanizadeh, S., and Li, L. Strain-rate-dependent nonlinear tensile properties of the superficial zone of articular cartilage. Connect Tissue Res **56,** 469, 2015.
72. Charlebois, M., McKee, M.D., and Buschmann, M.D. Nonlinear tensile properties of bovine articular cartilage and their variation with age and depth. J Biomech Eng **126,** 129, 2004.
73. Narmoneva, D.A. Direct measurement of the poisson's ratio of human patella cartilage in tension. J Biomech Eng **124,** 223, 2002.
74. Chahine, N.O., Wang, C.C.-B., Hung, C.T., and Ateshian, G.A. Anisotropic strain-dependent material properties of bovine articular cartilage in the transitional range from tension to compression. J Biomech **37,** 1251, 2004.
75. Elder, S., Chenault, H., Gloth, P., *et al.* Effects of antigen removal on a porcine osteochondral xenograft for articular cartilage repair. J Biomed Mater Res A **106,** 2251, 2018.
76. Schlichting, K.E., Copeland-Johnson, T.M., Goodman, M., *et al.* Synthesis of a novel photopolymerized

nanocomposite hydrogel for treatment of acute mechanical damage to cartilage. Acta Biomater **7,** 3094, 2011.
77. Buckley, M.R., Bonassar, L.J., and Cohen, I. Localization of viscous behavior and shear energy dissipation in articular cartilage under dynamic shear loading. J Biomech Eng **135,** 31002, 2013.
78. Nguyen, A.M., and Levenston, M.E. Comparison of osmotic swelling influences on meniscal fibrocartilage and articular cartilage tissue mechanics in compression and shear. J Orthop Res **30,** 95, 2012.
79. Buckley, M.R., Gleghorn, J.P., Bonassar, L.J., and Cohen, I. Mapping the depth dependence of shear properties in articular cartilage. J Biomech **41,** 2430, 2008.
80. Griffin, D.J., Bonnevie, E.D., Lachowsky, D.J., *et al.* Mechanical characterization of matrix-induced autologous chondrocyte implantation (MACI®) grafts in an equine model at 53 weeks. J Biomech **48,** 1944, 2015.
81. Middendorf, J.M., Griffin, D.J., Shortkroff, S., *et al.* Mechanical properties and structure-function relationships of human chondrocyte-seeded cartilage constructs after in vitro culture. J Orthop Res **35,** 2298, 2017.
82. Sennett, M.L., Meloni, G.R., Farran, A.J.E., Guehring, H., Mauck, R.L., and Dodge, G.R. Sprifermin treatment enhances cartilage integration in an in vitro repair model. J Orthop Res **36,** 2648, 2018.
83. Gilbert, S.J., Singhrao, S.K., Khan, I.M., *et al.* Enhanced tissue integration during cartilage repair in vitro can be achieved by inhibiting chondrocyte death at the wound edge. Tissue Eng Part A **15,** 1739, 2009.
84. Arvayo, A.L., Wong, I.J., Dragoo, J.L., and Levenston, M.E. Enhancing integration of articular cartilage grafts via photochemical bonding. J Orthop Res **36,** 2406, 2018.
85. Theodoropoulos, J.S., De Croos, J.N.A., Park, S.S., Pilliar, R., and Kandel, R.A. Integration of tissue-engineered cartilage with host cartilage: an in vitro model. Clin Orthop Relat Res **469,** 2785, 2011.
86. DiMicco, M.A., Patwari, P., Siparsky, P.N., *et al.* Mechanisms and kinetics of glycosaminoglycan release following in vitro cartilage injury. Arthritis Rheum **50,** 840, 2004.
87. Sitterle, V.B., Nishimuta, J.F., and Levenston, M.E. Photochemical approaches for bonding of cartilage tissues. Osteoarthritis Cartilage **17,** 1649, 2009.
88. Ahsan, T., and Sah, R.L. Biomechanics of integrative cartilage repair. Osteoarthritis Cartilage **7,** 29, 1999.
89. Peretti, G.M., Zaporojan, V., Spangenberg, K.M., Randolph, M.A., Fellers, J., and Bonassar, L.J. Cell-based bonding of articular cartilage: an extended study. J Biomed Mater Res A **64A,** 517, 2003.
90. Pabbruwe, M.B., Esfandiari, E., Kafienah, W., Tarlton, J.F., and Hollander, A.P. Induction of cartilage integration by a chondrocyte/collagen-scaffold implant. Biomaterials **30,** 4277, 2009.
91. Guidance for Industry: preparation of IDEs and INDs for products intended to repair or replace knee cartilage. Rockville, MD. 2011. Available at: https://www.fda.gov/media/82562/download. Accessed June 18, 2019.
92. Hurtig, M.B., Buschmann, M.D., Fortier, L.A., *et al.* Preclinical studies for cartilage repair: recommendations from the International Cartilage Repair Society. Cartilage **2,** 137, 2011.
93. International ASTM. ASTM F2451-05(2010) Standard Guide for In Vivo Assessment of Implantable Devices Intended to Repair or Regenerate Articular Cartilage (2010). 2005.
94. Moutos, F.T., and Guilak, F. Functional properties of cell-seeded three-dimensionally woven poly(ε-caprolactone) scaffolds for cartilage tissue engineering. Tissue Eng Part A **16,** 1291, 2010.
95. Gonzalez, J.S., and Alvarez, V.A. Mechanical properties of polyvinylalcohol/hydroxyapatite cryogel as potential artificial cartilage. J Mech Behav Biomed Mater **34,** 47, 2014.
96. Pfeifer, C.G., Fisher, M.B., Carey, J.L., and Mauck, R.L. Impact of guidance documents on translational large animal studies of cartilage repair. Sci Transl Med **7,** 310re9, 2015.
97. Lyyra, T., Jurvelin, J., Pitkänen, P., Väätäinen, U., and Kiviranta, I. Indentation instrument for the measurement of cartilage stiffness under arthroscopic control. Med Eng Phys **17,** 395, 1995.
98. Duda, G.N., Kleemann, R.U., Bluecher, U., and Weiler, A. A new device to detect early cartilage degeneration. Am J Sports Med **32,** 693, 2004.
99. Kiviranta, P., Lammentausta, E., Töyräs, J., Kiviranta, I., and Jurvelin, J.S. Indentation diagnostics of cartilage degeneration. Osteoarthritis Cartilage **16,** 796, 2008.
100. Wang, L., Chen, S., An, K.-N., Yang, H.-L., and Luo, Z.-P. Theoretical prediction of ultrasound elastography for detection of early osteoarthritis. ScientificWorldJournal **2013,** 565717, 2013.
101. Tang, S.Y., Souza, R.B., Ries, M., Hansma, P.K., Alliston, T., and Li, X. Local tissue properties of human osteoarthritic cartilage correlate with magnetic resonance T(1) rho relaxation times. J Orthop Res **29,** 1312, 2011.
102. Boskey, A., and Pleshko Camacho, N. FT-IR imaging of native and tissue-engineered bone and cartilage. Biomaterials **28,** 2465, 2007.
103. Nieminen, H.J., Zheng, Y.P., Saarakkala, S., *et al.* Quantitative assessment of articular cartilage using high-frequency ultrasound: research findings and diagnostic prospects. Crit Rev Biomed Eng **37,** 461, 2009.

Address correspondence to:
Robert L. Mauck, PhD
McKay Orthopaedic Research Laboratory
Perelman School of Medicine
University of Pennsylvania
308A Stemmler Hall
3450 Hamilton Walk
Philadelphia, PA 19104-6081

E-mail: lemauck@pennmedicine.upenn.edu

Received: April 25, 2019
Accepted: July 1, 2019
Online Publication Date: September 30, 2019